Separation Science and Technology
Publication details, including instructions for authors and subscription information:
http://www.informaworld.com/smpp/title~content=t713708471

Steady-State Characteristics of Lithium Isotope Separation by a Circuit of Continuous Displacement Chromatography

S. Fujine[a]; K. Saito[a]; K. Shiba[a]; T. Itoi[b]
[a] Division of Nuclear Fuel Research, Japan Atomic Energy Research Institute Tokai, Ibaraki, Japan [b] Speciality Products Laboratory, Mitsubishi Chemical Industries Limited Research Center, Yokohama, Kanagawa, Japan

To cite this Article Fujine, S. , Saito, K. , Shiba, K. and Itoi, T.(1982) 'Steady-State Characteristics of Lithium Isotope Separation by a Circuit of Continuous Displacement Chromatography', Separation Science and Technology, 17: 13, 1545 — 1563

To link to this Article: DOI: 10.1080/01496398209438472

URL: http://dx.doi.org/10.1080/01496398209438472

SEPARATION SCIENCE AND TECHNOLOGY, 17(13 & 14), pp. 1545–1563, 1982-83

Steady-State Characteristics of Lithium Isotope Separation by a Circuit of Continuous Displacement Chromatography

---

S. FUJINE, K. SAITO, and K. SHIBA

DIVISION OF NUCLEAR FUEL RESEARCH
JAPAN ATOMIC ENERGY RESEARCH INSTITUTE
TOKAI, IBARAKI, JAPAN

T. ITOI

SPECIALITY PRODUCTS LABORATORY
MITSUBISHI CHEMICAL INDUSTRIES LIMITED RESEARCH CENTER
YOKOHAMA, KANAGAWA, JAPAN

Abstract

Height equivalent to a theoretical plate (HETP), which is an important factor to determine separation performance, is experimentally obtained for lithium isotope separation by a circuit of continuous displacement chromatography. The values of HETP are related to the flow rates and concentrations of the displacement reagents. A new equation to estimate HETP is derived and shows good agreement with the experimental data. Diffusion in the resin is found to be the major resistance for the isotope exchange reaction, and liquid mixing in the columns also strongly influences the value of HETP.

INTRODUCTION

Lithium isotope separation is carried out by continued displacement of a band in ion-exchange columns. We have reported that the separation characteristics of displacement chromatography are well explained by the theories of square cascades (*1*, *2*), and indicated that Glueckauf's chromatographic theoretical stages (*3*) had about twice the height of a theoretical stage which would be obtained from the cascade model. Van Deemter (*4*), Giddings (5), Knox (*6–8*), and Snyder (*9*) also have presented their equations to estimate the height equivalent to a theoretical plate (HETP) for chromatography. But these equations are obtained for the elution technique and cannot be directly adapted to the present separation system. Since the HETP is an important factor to determine the isotope separation performance, we derive a new estimation equation by assuming a band to be a cascade in the steady state. The liquid mixing in columns is also considered in this equation.

Lithium isotope concentration profiles in the bands at the steady state are experimentally obtained by varying the operation conditions of a circuit. Furthermore, the effective diffusivities representing the liquid mixing are experimentally obtained. Then the new estimation equation of HETP is applied to these experimental data.

THEORY

In displacement chromatography the adsorption band moves with a fixed length and is assumed to be a square cascade or a distillation column in total reflux operation. The isotopes are separated in the moving band (*1*).

The height equivalent to a theoretical plate is defined as the height of a section of resin bed where the two streams leaving in the opposite directions are in equilibrium. The theoretical stage number can be found by applying Fenske's equation (*13*) to the isotope concentration profiles at the steady state. HETP is given as the length of the band divided by the theoretical stage number. The values of HETP are determined by the finiteness of interphase mass transfer coefficients and by liquid dispersion outside the resin particles.

At the steady state of isotope separation in the bands, the following relation holds:

$$\bar{N}_z = N_z \tag{1}$$

where $\bar{N}$ and N are the isotope fractions in the resin and liquid phases, respectively, as shown in Fig. 1, and the longitudinal distance z represents a theoretical plate which moves at the same speed u_B (cm/s) as the band. The material balance of the isotope is expressed for the resin phase of a thin layer δ_z;

$$L' \left(\bar{N}_z - \bar{N}_{z+\delta_z}\right) = -\,\delta_z q_0 A \left(\frac{d\bar{N}}{dt}\right)_z \tag{2}$$

namely, for the case where the cross-sectional area of the column A (cm^2) is unity:

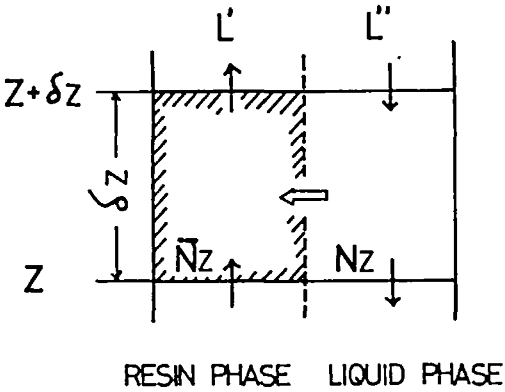

FIG. 1. Mass transfer in bands.

$$L'\left(\frac{\partial \bar{N}}{\partial z}\right)=q_0\left(\frac{\partial \bar{N}}{\partial t}\right) \tag{3}$$

where q_0 (mol/cm^3) is the ion exchange capacity and L' (mol/s) is the theoretical interstage flow rate:

$$L'=q_0u_B \tag{4}$$

Diffusion is the major resistance for the ion-exchange reaction. If the main resistance is exhibited inside the resin particles, the reaction rate may be approximated by a simple "linear-driving-force" relation, using the resin-phase mass transfer coefficient K_s (cm/s) and mass transfer area a (cm^2/cm^3-bed) between the phases, based on the concentrations in resin (*10*):

$$\frac{\partial \bar{N}}{\partial t}=K_sa(\bar{N}^*-\bar{N}) \tag{5}$$

where $\bar{N}^*$ is the equilibrium isotope fraction in resin. From Eqs. (3), (4), and (5),

$$dz=\frac{u_B}{K_sa}\,\frac{d\bar{N}}{\bar{N}^*-\bar{N}} \tag{6}$$

is derived. The concentration $\bar{N}$ varies from N_1 to N_2 as the distance z varies from 0 to z. Equation (6) is integrated to

$$z = \frac{u_B}{K_s a} \int_{N_1}^{N_2} \frac{d\bar{N}}{\bar{N}^* - \bar{N}} \tag{7}$$

The terms on the right-hand side of the equation are called in distillation theory:

$$\text{Height of a transfer unit (HTU)} = \frac{u_B}{K_s a} \quad \text{(cm)} \tag{8}$$

$$\text{Number of transfer units (NTU)} = \int_{N_1}^{N_2} \frac{d\bar{N}}{\bar{N}^* - \bar{N}} \quad (-) \tag{9}$$

The isotope separation factor α is defined by

$$\alpha = \frac{\bar{N}^*}{1 - \bar{N}^*} \bigg/ \frac{N}{1 - N} \tag{10}$$

The equation is changed to

$$\bar{N}^* = \frac{\alpha N}{1 + (\alpha - 1)N} \tag{11}$$

The NTU is obtained by the integration of Eq. (9) using Eqs. (1) and (11):

$$\text{NTU} = \int_{N_1}^{N_2} \frac{1 + (\alpha - 1)N}{\alpha N - N\{1 + (\alpha - 1)N\}} \, dN$$

$$= \frac{1}{\alpha - 1} \ln \frac{N_2}{N_1} \left(\frac{1 - N_1}{1 - N_2} \right)^{\alpha} \tag{12}$$

The equation also holds for large separation factors, as far as diffusion is the major resistance for the reactions (*11*). In the case of small isotope separation factors, $\alpha \approx 1$, Eq. (12) becomes the Fenske's equation using the approximation $\alpha - 1 \approx \ln \alpha$:

$$S = \frac{\ln \dfrac{N_2(1 - N_1)}{N_1(1 - N_2)}}{\ln \alpha} \tag{13}$$

NTU becomes equal to the theoretical stage number S, and HTU is expressed, using Eq. (7), by

$$\mathrm{HTU} = \frac{u_B}{K_s a} = \frac{z}{S} = \mathrm{HETP} \tag{14}$$

That is, HTU equals HETP.

A similar derivation also holds for the case where the dominating resistance for the ion-exchange reaction is in the boundary layer of the liquid phase surrounding the resin particles. The material balance of the isotope for the liquid phase of a thin layer δz (see Fig. 1) leads to

$$L'' \frac{\partial N}{\partial z} = \varepsilon C_0 \left(\frac{\partial N}{\partial t}\right)_z \tag{15}$$

where L'' (mol/s) equals L', and the cross-sectional area of the column is assumed to be unity. The reaction rate may be approximated by using the liquid-phase mass transfer coefficient K_L (cm/s), based on the concentrations in liquid:

$$\partial N/\partial t = K_L a(N - N^*) \tag{16}$$

The integration of Eq. (15), substituted by Eqs. (16) and (4), gives

$$z = \frac{q_0 u_B}{\varepsilon C_0 K_L a} \int_{N_1}^{N_2} \frac{dN}{N - N^*} \tag{17}$$

And the following relation for NTU is obtained,

$$\mathrm{NTU} = \frac{1}{\alpha - 1} \ln \left(\frac{N_2}{N_1}\right)^{\alpha} \left(\frac{1 - N_1}{1 - N_2}\right) \tag{18}$$

In case of $\alpha \approx 1$, Eq. (18) also can be approximated by Fenske's equation, and NTU becomes equal to the theoretical stage number S. The HTU is expressed by

$$\mathrm{HTU} = \frac{(q_0/\varepsilon C_0) u_B}{K_L a} = \frac{z}{S} = \mathrm{HETP} \tag{19}$$

In the case where the resistance of mass transfer in both phases cannot be neglected, the overall mass transfer coefficient K_T (cm/s) is used. The overall capacity coefficient $K_T a$ (s^{-1}) is expressed by

$$\frac{1}{K_T a} = \frac{1}{K_S a} + \frac{(q_0/\varepsilon C_0)}{K_L a} \tag{20}$$

Similarly, the overall HETP is expressed by

$$\text{HETP} = \frac{u_B}{K_T a} = \left\{ \frac{1}{K_S a} + \frac{(q_0/\varepsilon C_0)}{K_L a} \right\} u_B \tag{21}$$

This equation reveals the relation between mass transfer coefficients and HETP. However, the effect of liquid mixing in columns has not yet been considered.

Equation (21) gives infinite small values of HETP for very large mass transfer coefficients. Liquid mixing, however, occurs in the void of resin beds in practice, and gives rise to some differences in isotope concentration between the liquid and resin phases. The effective diffusivity E (cm^2/s) may be determined for evaluation of the liquid mixing (*12*) as follows:

$$E\frac{dN}{dz} = u(N_{z+\delta z} - N_z) \tag{22}$$

where u (cm/s) is the linear velocity of the fluid in the void of the resin beds and is related to the superficial velocity by $u = \bar{u}/\varepsilon$. The difference of isotope concentrations, $N_{z+\delta z} - N_z$, is made by liquid mixing. Assuming that the equilibrium relation of Eq. (11) holds between $N_{z+\delta z}$ and N_z, the length δz becomes HETP. Then

$$z = \frac{\varepsilon E}{\bar{u}} \int_{N_1}^{N_2} \frac{dN}{N - N^*} \tag{23}$$

is derived. The equation is similar to Eq. (17). The value of HETP contributed by liquid mixing may be evaluated by

$$\text{HETP} = \varepsilon E/\bar{u} \tag{24}$$

This term should be added to Eq. (21).

The rates of ion exchange are expressed by using Glueckauf's approximations (*3*) for particle diffusion control by

$$\left(\frac{\partial \bar{N}}{\partial t}\right)_z = \frac{\bar{D}}{0.071 r_0^2}(\bar{N}^* - \bar{N}) \tag{25}$$

and for boundary layer diffusion control in liquid by

$$q_0\left(\frac{\partial \bar{N}}{\partial t}\right)_z = \frac{3D}{2\delta r_0} C_0(N - N^*) \tag{26}$$

where r_0 (cm) is the particle radius, $\bar{D}$ (cm^2/s) is the self-diffusion coefficient of Li$^+$ ions in the particles, D (cm^2/s) is the molecular diffusion coefficient of the ions in liquid, and δ (cm) is the thickness of boundary layers surrounding the resin particles and is given experimentally by

$$\delta = \frac{0.2 r_0}{1 + 70 r_0 \bar{u}} \tag{27}$$

The relation

$$\left(\frac{\partial \bar{N}}{\partial t}\right)_z = \frac{\varepsilon C_0}{q_0}\left(\frac{\partial N}{\partial t}\right)_z \tag{28}$$

holds for the present system. The capacity coefficients are written as

$$K_S a = \frac{\bar{D}}{0.071 r_0^2} \tag{29}$$

$$K_L a = \frac{3D}{2\delta r_0 \varepsilon} \tag{30}$$

Moreover, the speed of the moving band is related to the superficial velocity by

$$u_B = \frac{C_0}{q_0 + \varepsilon C_0}\bar{u} \tag{31}$$

In conclusion, HETP is expressed by

$$\mathrm{HETP} = \left(\frac{C_0}{q_0 + \varepsilon C_0}\right)\frac{0.071 r_0^2}{\bar{D}}\bar{u} + \left(\frac{q_0}{q_0 + \varepsilon C_0}\right)\frac{0.133 r_0^2 \bar{u}}{D(1 + 70 r_0 \bar{u})} + \frac{\varepsilon E}{\bar{u}} \tag{32}$$

This equation reveals the influence of physicochemical properties on HETP of the isotope separation by displacement chromatography. The first term on the right-hand side is due to the slow diffusion in particles, the second to the slow diffusion in the boundary layer of the liquid, and the third to liquid mixing. The molecular diffusion coefficient in liquid is very small [of the order of 10^{-5} (cm^2/s)] compared with the effective diffusivities due to liquid mixing in columns. The contribution of longitudinal molecular diffusion on HETP can be eliminated for most cases. Equation (32) gives about half of an HETP value obtained by Glueckauf's equation (*4*).

EXPERIMENTS OF ISOTOPE SEPARATION

The circuit for continuous displacement chromatography was composed of 2 cm i.d. × 1 m Pyrex columns packed with Diaion SK116, sulfonated strong acid cation-exchange resin, ion-exchange capacity 2.66 meq/mL, and mean particle diameter 100 μm. The columns were kept at a temperature of 20°C (*13*).

The ion-exchange resins in the columns were conditioned to the H-form with regeneration using 2 *N* HCl and rinsing. A lithium band was formed on the resin bed and was moved by sodium acetate solution in the circuit until the steady state was attained. The solution which flowed out of a sampling valve was collected using a fraction collector and analyzed for concentration.

The superficial velocity in the columns and the concentration of the displacement reagent were changed in the experiments. These two experimental paramenters are related to the speed of the moving bands by Eq. (31). The length of the lithium band was set to be shorter than 1 m for rapid attainment of the steady state.

The Influence of Superficial Velocities

Lithium isotope separation was carried out for several superficial velocities at a constant concentration, 0.5 mol/L of the displacement reagent. The experimental conditions are shown in Table 1. The isotope concentration profiles obtained at the steady states show a linear relation on the semilogarithmic ordinates in Fig. 2. The effluent volume of the ordinate is in proportion to the distance in the bands. These profiles are explained by Fenske's equation (*13*). The slopes of the lines reflect the magnitude of isotope separation in a unit length of the bands. Since the experimental conditions (except the superficial velocities) were not changed, the separation factor was constant in these experiments. The separation factor has been found to be 1.0028 by breakthrough experiments (*2*). The void fraction of the resin bed is 0.35, and the slopes of the lines were converted to HETP values.

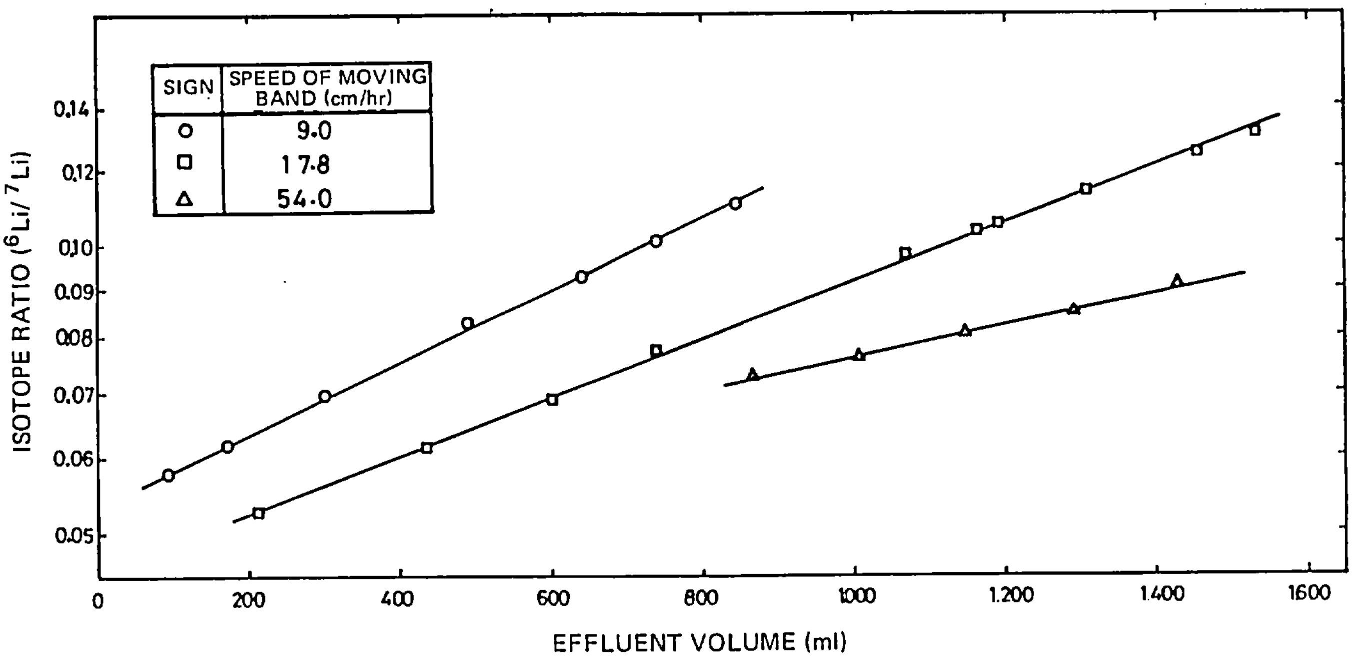

FIG. 2. Lithium isotope concentration profiles at the steady state.

TABLE 1
Experimental Conditions (effect of superficial velocity)

Run	Superficial velocity (m/h)	Speed of moving band (cm/h)	Band length (cm)
1	0.5	9.0	56.3
2	1.0	17.8	91.1
3	3.0	54.0	60.2

Figure 3 shows the linear relation of HETP to the speed of moving band. HETP increases from 0.18 to 0.40 cm when the speed of moving band increases from 9 to 54 cm/h, and may be expressed by

$$\mathrm{HETP} = 0.00489u_B + 0.136 \tag{33}$$

where the dimension of u_B is cm/h.

The Influence of Concentrations

Lithium isotope separation was carried out for several concentrations at a constant superficial velocity (1 m/h) of displacement reagent. The experimental conditions are shown in Table 2. The isotope concentration profiles obtained at the steady states are shown in Fig. 4. The slopes of the profiles decrease with increasing concentrations.

Lee reported that lithium isotope separation factors decreased with increasing concentrations (*14*). However, Hagiwara obtained an identical separation factor, 1.0036, for different concentrations, 0.2127 and 0.5858 mol/L (*15*). We also obtained the almost identical factor 1.0028 for the concentrations 0.3, 0.5, and 1.0 mol/L of lithium acetate by breakthrough experiments for the present system. Therefore, the isotope separation factors may be considered to be independent of the concentrations for these

TABLE 2
Experimental Conditions (effect of concentration)

Run	Concentration (mol/L)	Speed of moving band (cm/h)	Band length (cm)
1	0.3	11.8	59.8
2	0.5	17.8	91.1
3	1.0	33.8	56.7

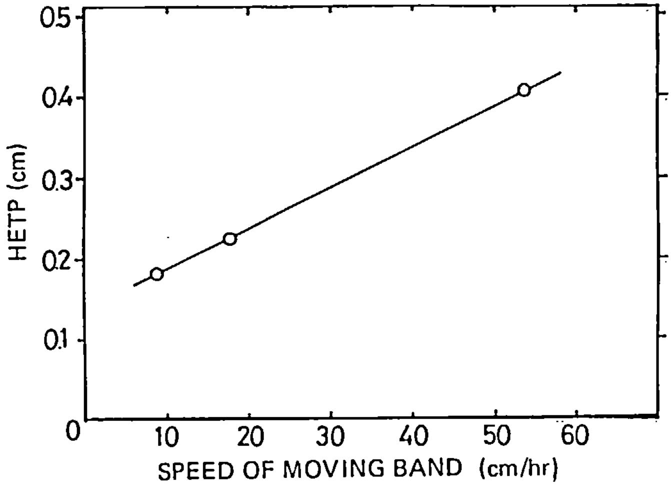

FIG. 3. Relation between HETP and the speed of the moving band. (Effect of superficial velocity.)

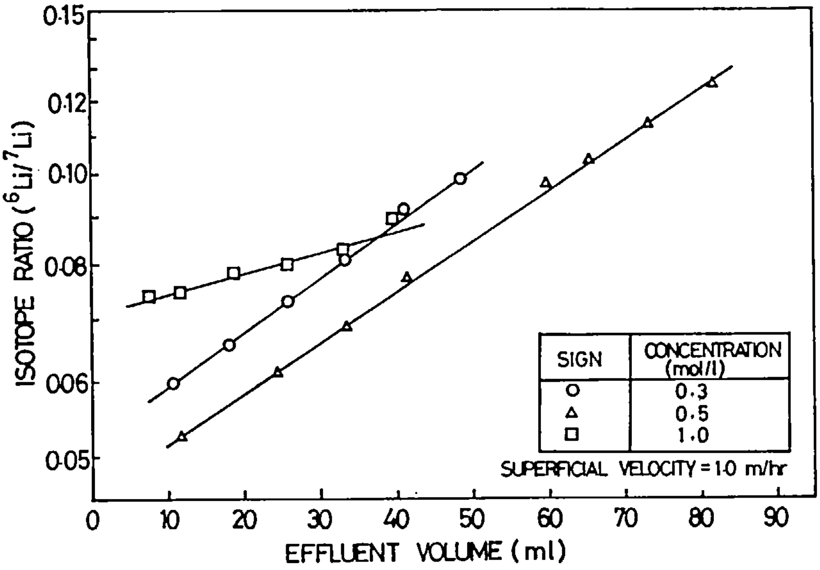

FIG. Fig. 4. Lithium isotope concentration profiles at the steady state.

displacement experiments. The HETP obtained varies with the concentrations as shown in Fig. 5 for the constant isotope separation factor of 1.0028.

The magnitude of isotope separation may be represented by the ratio of the isotopic ratios at arbitrary positions 10 cm apart. The factor equals α^s according to Fenske's equation, where s is the number of theoretical stages composing a 10-cm length of the band. Figure 6 shows the factors versus the speed of the moving bands. The magnitude of isotope separation per unit length is found to decrease with increasing speed of the moving bands. The extent depends on the experimental parameters. The separation factor is affected by concentrations rather than by superficial velocities.

The Boundaries of Bands

The following reactions occur at the front boundary of the lithium band:

$$R^- \, H^+ + Li^+ \rightleftharpoons R^- \, Li^+ + H^+ \quad (a)$$

$$H^+ + CH_3COO^- \rightleftharpoons CH_3COOH \quad (b)$$

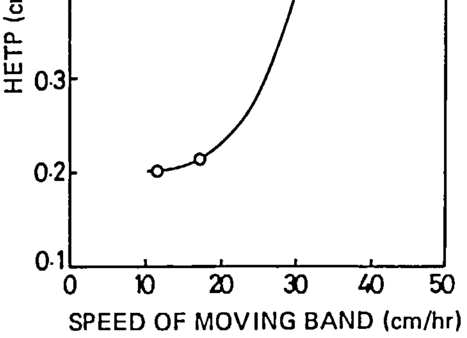

FIG. 5. Relation between HETP and the speed of the moving band. (Effect of concentration.)

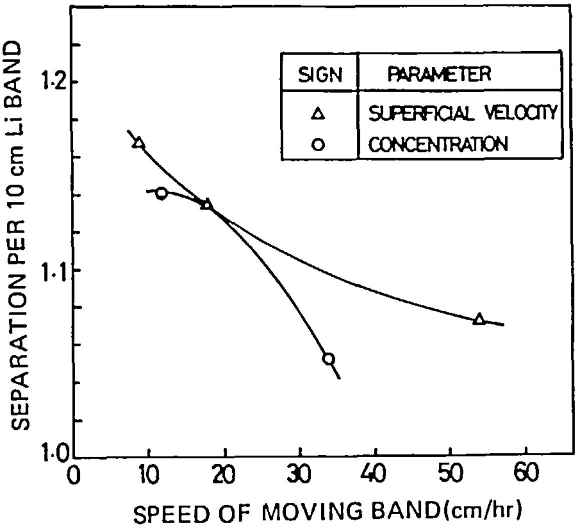

FIG. 6. The magnitude of separation per a 10-cm length of lithium band as a function of the speed of the moving band.

where R`is the ionic group in the resin. The combination of Reactions (a) and (b) is

$$R- H^+ + Li^+ + CH_3COO^- \overset{K \gg 1}{\rightleftharpoons} R- Li^+ + CH_3COOH \qquad (c)$$

The reaction at the rear boundary is

$$R- Li^+ + Na^+ \overset{K' > 1}{\rightleftharpoons} R- Na^+ + Li^+ \qquad (d)$$

The rates of ion-exchange Reactions (a) and (d) are controlled by mutual diffusion of ions in the resin particles. Reaction (b) is accelerated by the concentration of acetate ions.

Lithium concentration profiles at the boundaries of bands are determined by the selectivity coefficients between the neighboring ions and also by the rates of interphase mass transfer. The boundaries of the lithium bands tend to expand with the superficial velocity at a concentration. On the other hand, at a superficial velocity, increasing the concentration sharpens the front boundary and expands the rear one, as shown in Fig. 7. This indicates that

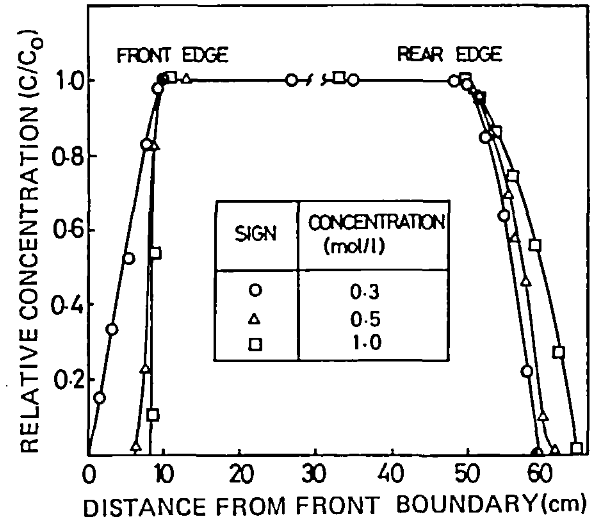

FIG. 7. Shapes of lithium adsorption bands.

the association Reaction (b) of acetate ions strongly affects the profiles at the front boundary.

EXPERIMENTS OF LIQUID MIXING

Liquid mixing occurs at various places in the circuit of displacement chromatography. The liquid mixing in the stagnant space above the resin bed can be observed directly from the patterns formed by two kinds of liquid of different refractive indices. "Fingering" and "tilting" are also observed through Pyrex walls, while the visible boundaries of bands move in the columns. The effect of liquid mixing may be treated using a diffusion model (*12, 16*). The effective diffusivities of axial direction in columns can be obtained by applying one-dimensional diffusion theory. Consider that a stepwise concentration change occurs at time $t = 0$ at the entrance of a column in which liquid flows at a constant linear velocity u (cm/s) in the bed. In the case of plug flow, the boundary between different concentrations moves at the speed of u (cm/s). However, assuming the effective diffusivity E (cm^2/s) in the column, the boundary disperses in accordance with

$$\frac{\partial c}{\partial t} = E\frac{\partial^2 c}{\partial x^2} - u\frac{\partial c}{\partial x} \tag{34}$$

where x (cm) is the distance from the entrance of the column. Danckwerts developed a mixing theory for packed columns (*12*) and derived the following equation for columns of length L (cm):

$$2\frac{C}{C_0} = 1 - \operatorname{erf}\left(\frac{1 - \dfrac{vt}{V}}{2\sqrt{\dfrac{vtE}{VLu}}}\right) \tag{35}$$

where V (cm^3) is the total void volume in a column, v (cm^3/s) is the flow rate, and C_0 (mol/L) is the concentration at the entrance at $t > 0$. The ratio C/C_0 is defined as the F-value, and plots of the F-value versus the dimensionless factor (vt/V) are called F-diagrams. Equation (35) indicates that the factor (E/Lu) determines the F-diagram. The effective diffusivities can be found from the slopes at $vt/V = 1$ of F-diagrams.

We obtained the stepwise response curves for a 2-cm i.d. × 1 m Pyrex

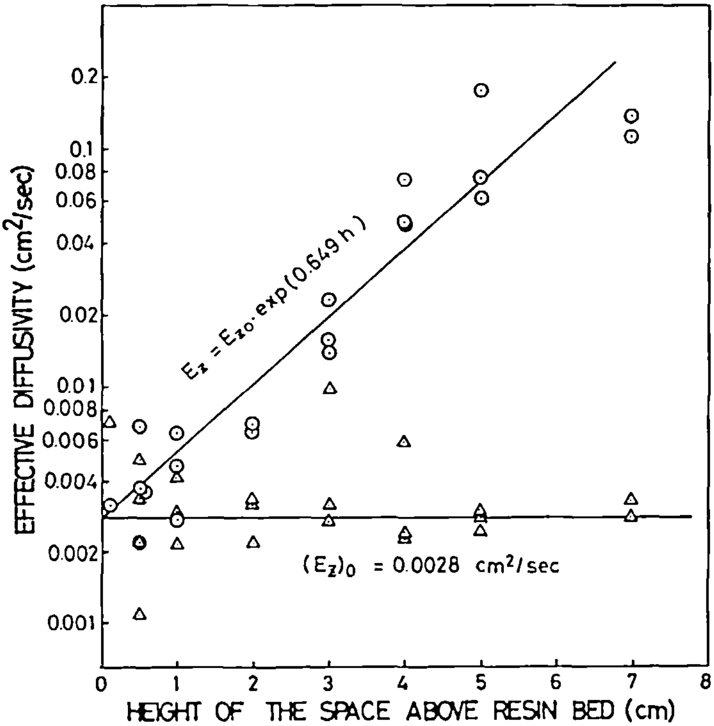

FIG. 8. Effective diffusivity representing the magnitude of liquid mixing in columns.

column packed with a Na-form of ion-exchange resin, Diaion SK116 (100 μm). Pure water and dilute NaCl solution were used, and the concentration changes were measured at the exit by an electric conductivity meter. Figure 8 shows the effective diffusivities obtained as a function of height of the space h (cm) above the resin bed for the superficial velocity of 3.0 m/h. When the fluid is changed from pure water to the NaCl solution, the diffusivities obtained increase with the height of the space. When the fluid is changed from the NaCl solution to pure water, however, the diffusivities do not depend on the height. This phenomenon is caused by a slight difference in liquid density. The boundary between the adjacent fluids is not disturbed in the space above the resin bed for the latter case. The value of effective diffusivity is found to be 0.0028 cm^2/s at 0 cm height of the space, which represents liquid mixing in the resin bed, i.e., fingering, tilting, and wall effects, including molecular diffusion, in the void of the column.

The effective diffusivities increase proportionately with the superficial velocity as Helfferich has indicated (*17*). Therefore, the effective axial diffusivities are expressed by

$$E = 0.034\bar{u} \exp(0.65h) \tag{36}$$

for the present experiments.

DISCUSSION

In general, the equations to estimate HETP for liquid chromatography have not exhibited agreement with experimental data (*17*). The causes are considered to exist in the complicated effects of liquid mixing and in the uncertainties of particle size distribution and diffusion coefficients in the particles. Accurate HETP should be obtained by experiments for individual separation systems.

Our Eq. (32) was applied to estimate HETP for the present experiments. The following conditions were used for calculation: particle radius of ion exchange resin, $r_0 = 0.005$ cm; ion exchange capacity, $q_0 = 2.66$ meq/mL; void fraction of the beds, $\varepsilon = 0.35$; self-diffusion coefficient of Li^+ ions in the resin particles, $\bar{D} = 1 \times 10^{-7}$ cm^2/s; and diffusion coefficient of Li^+ ions in liquid, $D = 1 \times 10^{-5}$ cm^2/s.

Figure 9 shows the effects of superficial velocities of HETP calculated by Eq. (32). The term for diffusion in particles is found to be about 10 times that of the term for diffusion in the boundary layer. Therefore, diffusion in particles is the major resistance to the isotope exchange reaction. These terms increase with superficial velocities, but the liquid mixing term gives a

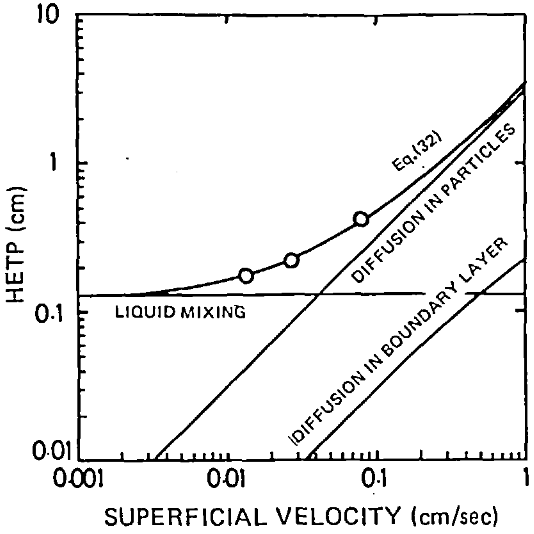

FIG. 9. Influence of superficial velocity on HETP.

constant value, 0.13 cm, which is obtained by using the effective diffusivities of Eq. (36) for the height, 3.7 cm, of the space above the resin bed in a 1-m long column. The value of the height was measured for the columns in the displacement chromatography circuit. The experimental data of HETP show a close agreement with those estimated by the equation. The effect of liquid mixing is found to be very large, and is almost equal to that of diffusion in particles.

Figure 10 shows the effects of concentrations on HETP calculated by Eq. (32). The term for diffusion in the boundary layer gives values smaller than 0.01 cm. The experimental data show some fluctuation from Eq. (32). The magnitude of the effect of liquid mixing is considered to depend on the concentrations of the displacement reagent.

CONCLUSION

An equation to estimate HETP was newly derived for lithium isotope separation by displacement chromatography, assuming the steady state in the bands. The isotope concentration profiles at the steady state were experimentally obtained by varying the operation conditions of a circuit. The magnitude of isotope separation per unit length of the band was found to decrease with increasing speed of the moving bands. The extent is more

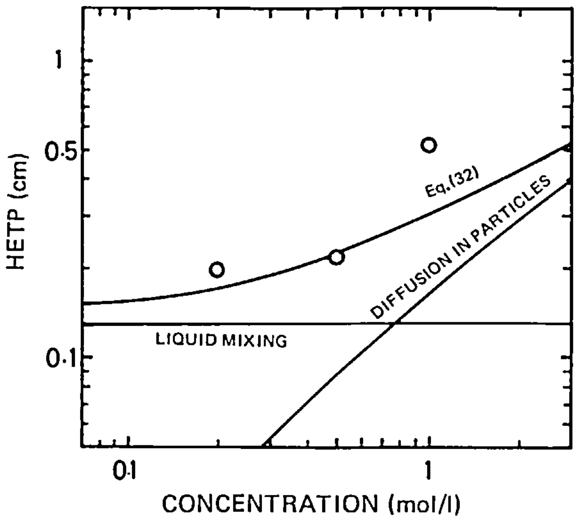

FIG. 10. Influence of concentration on HETP.

affected by the concentrations than by the superficial velocities of the displacement reagents. The effective diffusivities representing liquid mixing in columns were also experimentally obtained. Then the values of HETP were estimated for the present experimental conditions by our estimation equation. This equation was found to agree well with the experimental data. Moreover, diffusion in the resin was found to be the major resistance for the interphase isotope exchange reaction, and the liquid mixing in columns also strongly influenced the value of HETP.

Acknowledgments

The authors wish to express their appreciation to Prof Jun Ōishi of Kyoto University for many helpful discussions, and to Drs J. Shimokawa and K. Iwamoto of the Japan Atomic Energy Research Institute for encouragement and guidance.

REFERENCES

1. S. Fujine, *Sep. Sci. Technol.* *17*(8), 1049 (1982).
2. S. Fujine, K. Saito and K. Shiba, *Ibid.*, *17*(11), 1309 (1982).
3. E. Glueckauf, *Ion Exchange and Its Applications*, Soc. Chem. Ind., London, 1955, p. 34.

4. J. J. Van Deemter, F. J. Zuiderweg, and A. Klinkerberg, *Chem. Eng. Sci.*, *5*, 271 (1956).
5. J. C. Giddings and K. L. Mallik, *Anal. Chem.*, *38*(8), 997(1966).
6. G. J. Kennedy and J. H. Knox, *J. Chromatogr. Sci.*, *10*(9), 549(1972).
7. E. Grushka, L. R. Snyder, and J. H. Knox, *Ibid.*, *13*(1), 25(1975).
8. J. H. Knox, *Ibid.*, *15*(9), 352(1977).
9. L. R. Snyder, *Ibid.*, *7*(6), 352(1969).
10. T. K. Sherwood, R. L. Pigford, and C. R. Wilke, *Mass Transfer*, McGraw-Hill, New York, 1975, p. 548.
11. M. Van Winkle, *Distillation*, McGraw-Hill, New York, 1967, p. 604.
12. P. V. Danckwerts, *Chem. Eng. Sci.*, *2*(1), 1(1953).
13. S. Fujine, K. Saito, Y. Naruse, K. Shiba, M. Kosuge, T. Itoi, and T. Kitsukawa, JAERI-M 9735, 1981.
14. D. A. Lee and J. S. Drury, *J. Inorg. Nucl. Chem.*, *27*, 1405(1965).
15. Z. Hagiwara and Y. Takakura, *J. Nucl. Sci. Technol.*, *6*(5), 279(1969).
16. H. Brenner, *Chem. Eng. Sci.*, *17*, 229(1962).
17. F. Helfferich, *Ion Exchange*, McGraw-Hill, New York, 1962, p. 449.

Received by editor May 14, 1982